Jyoti Mayadev
Stanley H. Benedict
Mitchell Kamrava *Editors*

Handbook of Image-Guided Brachytherapy

Springer

Handbook of Image-Guided Brachytherapy

Jyoti Mayadev
Stanley H. Benedict
Mitchell Kamrava
Editors

Handbook of Image-Guided Brachytherapy

Springer

Editors
Jyoti Mayadev, MD
Associate Professor
Director of Brachytherapy
Department of Radiation Oncology
University of California Davis Medical Center
UC Davis Comprehensive Cancer Center
Sacramento, CA, USA

Mitchell Kamrava, MD
Assistant Clinical Professor
Chief, Division of Brachytherapy
Chief, Gynecologic and Sarcoma Services
Department of Radiation Oncology
University of California, Los Angeles
Los Angeles, CA, USA

Stanley H. Benedict, PhD, FAAPM
Professor and Vice Chair of Clinical Physics
Department of Radiation Oncology
University of California Davis Medical Center
UC Davis Comprehensive Cancer Center
Sacramento, CA, USA

ISBN 978-3-319-44825-1 ISBN 978-3-319-44827-5 (eBook)
DOI 10.1007/978-3-319-44827-5

Library of Congress Control Number: 2016959498

Printed on acid-free paper

This Springer imprint is published by Springer Nature
The registered company is Springer International Publishing AG
The registered company address is: Gewerbestrasse 11, 6330 Cham, Switzerland

Dedicated to the mentors, practitioners, and students of brachytherapy, who continually strive for innovation, outcome improvement, and a better patient experience. I am also deeply grateful to my loving parents (Savita and Shyam), supportive sisters (Renuka and Angeli), friends, and the collective universal spirit.

Jyoti Mayadev, MD

I would like to dedicate this handbook to my clinician and scientist friends for their enlightening and enduring contributions to radiation oncology, and for their tireless efforts to advance our clinical outcomes through

clinical research and development.
I am deeply indebted to the abiding and enduring love, support, and understanding from my family (Lori, Erin, and Noelle), which strengthens me and brings me joy and purpose beyond words.

Stanley H. Benedict, PhD, FAAPM

To my greatest teachers, Sophia and Sarah.

Mitchell Kamrava, MD

Preface

It is with great enthusiasm and dedication to the art and science of brachytherapy instruction, and on behalf of our authors, that we present our image-guided brachytherapy handbook. Brachytherapy is the use of radioactive sources placed near or into a tumor to provide a high radiation dose to the area of interest and a reduced dose to surrounding normal tissues. It is this therapeutic advantage and steep dose gradient falloff that continues to make brachytherapy one of the most conformal and long-standing treatments in cancer therapeutics. Throughout the last decade, the utility of image guidance in brachytherapy has increased to enhance procedural development, treatment planning, and radiation delivery in an effort to optimize safety and clinical outcomes. Given the complexity of image guidance and required incorporation into brachytherapy skillsets, the contents of this user-friendly handbook are designed to be a practical reference for the busy and dedicated clinician. Our goal is to provide a concise compilation of brachytherapy experiences at the reader's fingertip.

After formal training in brachytherapy by pioneers in the field, continuing friendship, kinship, and association with mentors and peers of brachytherapy, my clinical practice continues to evolve. With this collaboration and direction of specific and detailed knowledge, I recognize that not all practitioners have these individual educational opportunities and that a compilation of skills and "tips" should be made available to all brachytherapists and, in turn, to their collective patients.

This image-guided brachytherapy handbook is divided into two main parts: a radiobiology and physics section led by Dr. Stanley Benedict and a clinical site-specific section directed by Dr. Mitchell Kamrava and myself. The reader will learn about the rationale and background of brachytherapy in the first section, and then review the practical application of this modality in the second section. The handbook is a combination of outline text, procedural illustrations, contour examples, treatment planning techniques, and dosimetry for the comprehensive treatment for each disease site. The handbook answers practical questions regarding the incorporation of imaging advances such as CT, MRI, and ultrasound into brachytherapy procedures. Furthermore, it presents a detailed guide on how to extrapolate these technological advances into patient contours and treatment planning. Some examples of questions we sought to answer are:

- "How shall I use MRI or CT to help in my cervical cancer brachytherapy procedures or treatment planning?"
- "How could I implant a prostate using transrectal ultrasound or MRI guidance?"
- "How do I decide which breast brachytherapy technique is better for my patient: a single multichannel catheter vs an interstitial implantation?"

I am extremely grateful to a diverse team of brachytherapy experts who tirelessly devoted their time and innovative minds to the contents of this handbook. During the handbook preparation period, I was perpetually awestruck by our authors' ability to funnel their vast and substantial practical experiences into a concise and clinically relevant brachytherapy chapter. In addition, it continues to be an honor and pleasure to work in the field of brachytherapy and have developed this handbook with my coeditors, Drs. Stanley H. Benedict and Mitchell Kamrava, whose insight, knowledge, collaboration, and expertise are invaluable to our field.

Sacramento, CA, USA Jyoti Mayadev, MD

Contents

Contributors

Sushil Beriwal, MD Department of Radiation Oncology, University of Pittsburgh School of Medicine, Magee-Women's Hospital, Pittsburgh, PA, USA

Matthew Biagioli, MD, MSc Department of Radiation Oncology, University of Central Florida, Florida Hospital Cancer Institute, Orlando, FL, USA

Albert J. Chang, MD, PhD Department of Radiation Oncology, University of California, San Francisco, San Francisco, CA, USA

Jonathan Chen, MD, PhD Department of Radiation Oncology, New York Presbyterian Hospital/Weill Cornell Medicine, New York, NY, USA

J. Adam M. Cunha, PhD Department of Radiation Oncology, University of California, San Francisco, San Francisco, CA, USA

D. Jeffrey Demanes, MD, FACRO, FACR, FASTRO Division of Brachytherapy, Department of Radiation Oncology, UCLA David Geffen School of Medicine, Los Angeles, CA, USA

Brandon A. Dyer, MD Department of Radiation Oncology, Davis Comprehensive Cancer Center, University of California, Sacramento, CA, USA

Steven J. Frank, MD Department of Radiation Oncology, University of Texas MD Anderson Cancer Center, Houston, TX, USA

John Gloss, PSM Department of Radiation Oncology, Banner University Medical Center, University of Arizona, Tucson, AZ, USA

Karyn A. Goodman, MD, MS Department of Radiation Oncology, University of Colorado School of Medicine, Aurora, CO, USA

Dae Yup Han, PhD Department of Radiation Oncology, University of California, San Francisco, San Francisco, CA, USA

Alex Herskovic, MD Department of Radiation Oncology, New York Presbyterian Hospital/Weill Cornell Medicine, New York, NY, USA

I-Chow Hsu, MD, FACR, FASTRO Department of Radiation Oncology, University of California, San Francisco, San Francisco, CA, USA

Supriya K. Jain, MD, MHS Department of Radiation Oncology, University of Colorado School of Medicine, Aurora, CO, USA

Cameron Javid, MD, FACS Department of Ophthalmology, University of Arizona, Tucson, AZ, USA

Retina Associates, Tucson, AZ, USA

Mitchell Kamrava, MD Department of Radiation Oncology, University of California Los Angeles, UCLA Medical Plaza, Los Angeles, CA, USA

Taeho Kim, PhD Department of Radiation Oncology, Massey Cancer Center, Virginia Commonwealth University, Richmond, VA, USA

Rajat J. Kudchadker, PhD Department of Radiation Physics, University of Texas MD Anderson Cancer Center, Houston, TX, USA

Bruce Libby, PhD Department of Radiation Oncology, University of Virginia Health System, Charlottesville, VA, USA

Anna Likhacheva, MD, MPH Department of Radiation Oncology, Banner MD Anderson Cancer Center, Gilbert, AZ, USA

Justin Mann, MD Department of Radiation Oncology, New York Presbyterian Hospital/Weill Cornell Medicine, New York, NY, USA

Jyoti Mayadev, MD Department of Radiation Oncology, UC Davis Comprehensive Cancer Center, University of California Davis Medical Center, Sacramento, CA, USA

Amy C. Moreno, MD Department of Radiation Oncology, University of Texas MD Anderson Cancer Center, Houston, TX, USA

Alison Nielsen, MD Department of Anesthesiology and Pain Medicine, University of California, Davis Medical Center, Sacramento, CA, USA

Laura Padilla, PhD Department of Radiation Oncology, Virginia Commonwealth University Health System, Richmond, VA, USA

Bhupesh Parashar, MD Department of Radiation Oncology, New York Presbyterian Hospital/Weill Cornell Medicine, New York, NY, USA

Sang-June Park, PhD Department of Radiation Oncology, University of California, Los Angeles, Los Angeles, CA, USA

Shyamal Patel, MD Department of Radiation Oncology, University of California, Los Angeles, Lost Angeles, CA, USA

Jens Ricke, MD Department of Radiology and Nuclear Medicine, University of Magdeburg, Magdeburg, Germany

Kara D. Romano, MD Department of Radiation Oncology, University of Virginia Health System, Charlottesville, VA, USA

Kunal Saigal, MD Department of Radiation Oncology, Florida Hospital Cancer Institute, University of Central Florida College of Medicine, Orlando, FL, USA

Timothy N. Showalter, MD, MPH Department of Radiation Oncology, University of Virginia Health System, Charlottesville, VA, USA

Tijana Skrepnik, MD Department of Radiation Oncology, Banner University Medical Center, University of Arizona, Tucson, AZ, USA

Andrew W. Smith, BA University of Rochester School of Medicine and Dentistry, Rochester, NY, USA

Baldassarre Stea, MD, PhD Department of Radiation Oncology, Banner University Medical Center, University of Arizona, Tucson, AZ, USA

Shoshana Taube, BA Bar Elan Medical School, Ber Sheva, Israel

David H. Thomas, PhD Department of Radiation Oncology, University of Colorado Denver, Denver, CO, USA

Dorin A. Todor, PhD Department of Radiation Oncology, Virginia Commonwealth University Health System, Richmond, VA, USA

Daniel M. Trifiletti, MD Department of Radiation Oncology, University of Virginia Health System, Charlottesville, VA, USA

Andrew T. Vaughan, PhD Department of Radiation Oncology, Davis Medical Center, University of California, Sacramento, CA, USA

Jihong Wang, PhD Department of Radiation Physics, University of Texas MD Anderson Cancer Center, Houston, TX, USA

A. Gabriella Wernicke, MD, MS Department of Radiation Oncology, New York Presbyterian Hospital/Weill Cornell Medicine, New York, NY, USA

Yao Yu, MD Department of Radiation Oncology, University of California, San Francisco, San Francisco, CA, USA

Xiao Zhao, MD Department of Radiation Oncology, Davis Medical Center, University of California, Sacramento, CA, USA

Part I
Radiobiology and Physics of Image-Guided Brachytherapy

Chapter 1
Radiobiology of Brachytherapy

Xiao Zhao and Andrew T. Vaughan

Basic Radiobiological Principles

DNA Damage

- Radiation therapy exerts its effects primarily through DNA damage mediated by either direct deposition of energy within DNA (~40 %) or secondarily through the generation of free radicals (~60 %)
- The free radicals may subsequently attack DNA and generate both DNA breaks and/or mutations. However, both free radical access may be restricted by the presence of chemical scavengers, such as glutathione, and chemical fixation of lesions is reduced in regions of low oxygen tension

X. Zhao, MD • A.T. Vaughan, PhD (✉)
Department of Radiation Oncology, Davis Medical Center, University of California, 4501 X Street, Sacramento, CA 95817, USA
e-mail: jazhao@ucdavis.edu; atvaughan@ucdavis.edu

J. Mayadev et al. (eds.), *Handbook of Image-Guided Brachytherapy*, DOI 10.1007/978-3-319-44827-5_1

Cell Death

- The discrete, localized, disruption of DNA generates double strand breaks that may combine with breaks on other chromosomes to produce lethal lesions that physically disrupt cell division
- Such lesions that limit cell division include chromosome rearrangements with two centromeres, a dicentric, that restricts the ability of the cell to divide. For this reason, this type of lethality is called a mitotic cell death or mitotic catastrophe and is prominent in the cells of most irradiated carcinoma
- Radiation-induced apoptosis is less common but may be observed under certain conditions, such as in endothelial cells after large single doses [1]
- Generating a lethal lesion that will lead to cell death is of key significance for both tumor control and the maintenance of normal tissues

DNA Damage Tracking

- The formation of DNA double stand breaks by irradiation may be tracked by the phosphorylation of serine 139 of multiple H2AX histones that surround the break itself
- The appearance and then removal of γH2AX phosphorylation tracks with reasonable accuracy the survival changes measured with sublethal damage repair (SLDr) consistent with their being a link between them [2]

Linear Quadratic Equation

- The required sublesions may be generated either from the same radiation event or separately. Using this understanding, the survival curves of irradiated cells

have been modeled by a two component polynomial where the fraction surviving (SF) a dose (d) includes a linear component (αD) representing the simultaneous generation of DNA breaks and a quadratic component (βD^2) where the breaks are introduced as separate events

- Thus, the Linear Quadratic (LQ) equation takes the form:

$$SF = e^{-(\alpha d + \beta d^2)} \quad (1)$$

- The LQ equation therefore is more than a simple curve fitting routine in that it is based on a biological assessment of how radiation kills cells
- The relevance (or lack thereof) of the LQ relationship at large single doses (>10 Gy) is a matter of some dispute and will be discussed later
- In clinical practice, the LQ equation has often been used to estimate the effects of fraction size changes on tumor killing and tissue toxicity

Dose–Response Curves

- The shapes of acute (most tumors) and chronically (most normal tissues and some tumors such as prostate) responding tissues is quite different with the acutely responding dose response being flattened with less curvature than the chronic responders (Fig. 1.1)
- The different shapes of the dose–response curves have one immediate impact. As the dose delivered increases, the effect on late responding tissues gets progressively more significant as the dose–response curve continues to bend. Thus, large fractions delivered to critical normal tissues are to be avoided for this reason

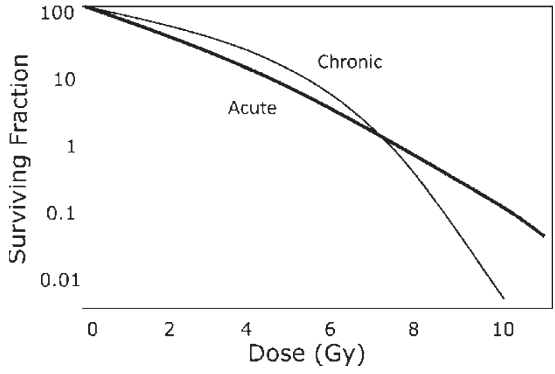

FIG. 1.1. Cell survival curves. The shapes of these two curves illustrate the predicted increased response to fraction size for chronically responding (normal tissues) targets compared to acute responders (most tumors). The difference is encapsulated in a single unit of dose, the α/β ratio derived from the linear quadratic equation where killing from the αD component equals that from the βD^2 component. Its value is high (~10 Gy) for acute responding tissues and low (~3 Gy) for most chronic reactions

Survival Curve Analysis: The α/β Ratio

- In order to provide a simple index of what constitutes an acute or chronic dose response, a unique single dose is defined where the contribution to cell killing from single event killing (αD) exactly matches that from the combination of two separate events (βD^2). This is known as the α/β ratio and is measured in dose units
- For acutely responding tissues (most tumors), the αD component predominates thus the α/β ratio equivalence point is not reached until quite high doses. Conversely, the more curved chronically responding tissues that describe most normal tissues the curved element is greater, and the equivalence point is lower

- By convention, and unless the actual numbers are determined by experiment, acute responding tissues are commonly assigned an α/β ratio of 10 Gy and chronic responders an α/β ratio of 3 Gy

The Differences Between External Beam Radiation Therapy and Brachytherapy

Brachytherapy Applications

- Brachytherapy by definition is radiation therapy in which a radioactive source is placed within or in close proximity to the area being treated.
- Traditional sites that have been treated with brachytherapy include gynecological cancers, prostate cancer, head and neck cancers, and skin cancers
- The central location of cervical tumors and their relative accessibility made brachytherapy the treatment of choice, initially using radium as the primary radiation source
- Very high, and steep dose gradients, close to the radiation source contributes to dose and dose rate heterogeneity that is not normally observed using external beams. This can be difficult to account for using traditional normal tissue tolerances
- Treatment with linear accelerators usually operates within a certain dose rate delivery range and treatment completes within minutes. However, the dose rate in brachytherapy varies from permanent implants delivering dose over months to short high dose delivery treatments in minutes. This can produce significantly different radiobiological effects

Dose Rates

- Multiple strategies have been used that are traditionally defined by the dose rate (DR) delivered. These include Very Low (VLDR <40 cGy h^{-1}), Low (LDR

<2 Gy h^{-1}), Medium (MDR 2Gy–12 Gy h^{-1}), High (HDR >12 Gy h^{-1}), and Pulsed (PDR ~ hourly)

- Modern day brachytherapy is, however, most often classified into two categories: HDR brachytherapy vs. LDR brachytherapy
- HDR is typically used to describe catheter-based procedures using non-permanent radioactive sources that complete treatment in minutes
- LDR is typically used to describe permanent implants that by definition will provide a continuous, decreasing, dose rate to the target
- Pulsed Dose Rate (PDR) Brachytherapy was designed to deliver several small HDR fractions over a shorter interval (<3–4 h) to capture more DNA lesions prior to repair, thus providing similar biologic effects to traditional LDR treatments

Radiobiological Effect of Different Dose Rates

- Alterations in the rate of dose delivery within the range likely to be encountered in the clinic have a substantial impact on cell survival
- For most tumor types irradiated in vitro, as the dose rate is decreased below ~100 cGy min^{-1} the effectiveness of the irradiation is incrementally decreased, as demonstrated by the standard clonogenic survival curve
- It is likely that all of the factors that are known to modulate the response of cells to irradiation, including the 4(5) "R's" (see below), will have some effect on both tumors and normal tissues [3] (Fig. 1.2)
- However, of these, it is the capacity to repair DNA damage and the potential for reoxygenation that are likely to show most variability during different brachytherapy protocols

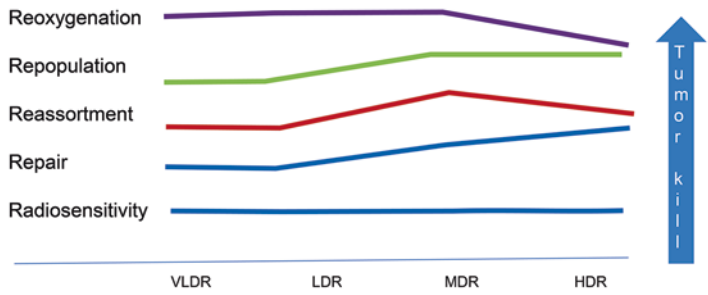

FIG. 1.2. Schematic illustrating the relative impact of brachytherapy delivery technique on biological response. Reoxygenation may be decreased if few large doses used. Repopulation of tumor will occur if small doses are delivered over a protracted period. The Reassortment of cells within the cell cycle into the more radiosensitive G_2M phase will happen at unique dose rates, but is difficult to predict clinically. Decreasing dose rates will enhance Repair and therefore survival. Decreasing dose rate will also enhance the expression of any differential Radiosensitivity, primarily through differences in DNA repair, though any specific benefit is difficult to predict

The 4(+1) "R's" of Radiobiology: Repair, Reoxygenation, Redistribution, Repopulation (and Radiosensitivity)

Repair

- The requirement for two DNA breaks, or sublesions, to generate the lethal event also provides the setting for their repair. Thus, if the individual breaks occur separated in time and/or space then one may be repaired before it has the opportunity to interact with the other
- The significance of this type of repair, called "sublethal damage repair" or SLDr, is clear in that through its activity fewer lesions will be produced if the dose is fractionated or delivered at a lower dose rate such that individual lesions are repaired and therefore cannot react with other lesions to generate a lethal event

- DNA sublethal lesions are removed by active DNA repair systems, primarily the error prone Non Homologous End Joining (NHEJ) or Homologous Recombination (HR) repair. In the latter case, increased repair fidelity is provided by using the intact homologous copy of the damaged sequence to template the repair
- The impact of the extremes of dose rate delivery is easy to describe. At very low dose rate ~0.4 cGy min^{-1} or less, such as might be observed after substantial decay of a permanent seed implant, DNA breaks have the greatest chance to be successfully repaired (few alternative breaks for interaction) and minimal toxicity will occur
- At high dose rates ~100 cGy min^{-1} and above, DNA breaks will have the greatest chance to combine with other breaks, potentially generating a lethal lesion and thus reduced survival
- Dose rates that fall between these extremes will provide an intermediate level of lethal lesion generation depending on the delivery parameters and the repair capability of the target tissue

Reoxygenation

- Multiple studies have shown that most animal and human tumors contain regions of lowered oxygen tension where the blood supply network has not kept pace with the expansion of the tumor volume
- Classical studies in radiobiology have shown that such regions of hypoxia reduce the effectiveness of irradiation by limiting the fixation of free radical damage that is best achieved in the presence of molecular oxygen
- The reduction in radiation effect is significant, approximately three fold when comparing irradiation under oxic or hypoxic conditions

- This difference is sufficiently large that it would render radiation therapy ineffective unless reoxygenation occurs during treatment
- As well-oxygenated cells die from radiation damage, hypoxic cells may have improved access to the blood supply and become more sensitive to future radiation treatments. This process can begin rapidly after treatment
- Considering the wide variation in treatment schedules that may occur within brachytherapy, it is difficult to predict the impact of hypoxia on cell kill for small variations in the rate and time of dose delivery
- However, large treatment doses that are delivered rapidly over a short time frame are least likely to ensure complete reoxygenation as the residual tumor mass may still metabolize oxygen—limiting its access to hypoxic regions

Redistribution

- Acute radiation exposures will kill the most sensitive cell populations, specifically those in $G_2M > G_1$ early S > late S. The residual viable cells will then be partially synchronized
- Transition through the cell cycle is linked to checkpoints, which may be activated by genomic damage, which will provide a pause to allow DNA damage repair
- Activation of the G_2M checkpoint during a protracted exposure at a dose rate of ~0.5–1 cGy min^{-1} will stall cells at this very radiation sensitive phase of the cell cycle generating more cell kill if the dose continues
- Paradoxically, higher dose rates, ~1–2 cGy min^{-1} or greater, will freeze the progression of cells through the cell cycle such that some will remain in a relatively resistant part of the cell cycle. Here, such cells will

survive better than those irradiated at a slightly lower dose rate, ~0.5 cGy min^{-1}, that may proceed through to the radiosensitive G_2M arrest point, and continue to be irradiated. This unusual feature is called the "inverse dose rate effect."

- Interestingly, one of the original applications of brachytherapy for cervical tumors used interstitial radium implants delivering a dose rate of ~40 cGy h^{-1}. This dose rate is consistent with the inverse dose rate effect described, potentially contributing to the efficacy of this treatment method

Repopulation

- After protracted exposure to radiation, residual tumor cells may increase their rate of cell division. This is one of the principle reasons why delays in any protracted irradiation schemes are to be avoided
- This parameter was initially described by key studies of Withers et al. Here, in a head and neck cancer setting, the dose to achieve tumor control (TCD_{50}) increased after 30 days of treatment [4]. The explanation for this finding was the accelerated repopulation of tumor clonogens
- The effect of repopulation is related more to total treatment duration than dose rate. This effect is not seen in treatment delivery times less than 1 week. After 1 week, there can be increased repopulation of high turnover normal tissues such as the skin and mucosa. For treatment delivery times greater than 3 weeks, there could be repopulation effects of fast growing tumors
- In terms of brachytherapy, faster treatments will mitigate this effect. However, faster treatment times may limit successful reoxygenation of the tumor—how this balance impacts outcome within the same or different tumor types is not known

Radiosensitivity

- Individual tumor types vary substantially as to their response to irradiation. Thus, clonogens from a radiation unresponsive tumors are also likely to be radiation resistant; however, this is only one factor in the ability of radiation to control an individual tumor [5]
- The role of radiation sensitivity followed a number of studies that showed a correlation between the radiation response of individual tumor types and the in vitro clonogenic sensitivity of their tumor cells, particularly as measured by the fraction surviving 2 Gy (SF_2) [6]
- The relative differences in tumor cell survival after irradiation is reduced at higher doses as the slopes of the survival curves become increasingly similar
- Thus, relative differences in intrinsic radiation sensitivity, either between tumors of the same type or between tumors with different radiation response profiles, may be of lesser importance following large doses of brachytherapy than multiple smaller doses of conventional (1.8–2 Gy) fractionation

How Are 4R(5)s Affected by the Interval Between Fractions?

- Repair—Most repair happens between the first few hours after irradiation so unless a very short interval is used between fractions such as in PDR, the interval between fractions will not affect the degree of repair
- Redistribution—There is likely no measurable clinical impact of redistribution, based on the interval between fractions, due to the clonal heterogeneity of tumor composition
- Repopulation—As discussed previously, this effect typically does not occur until after 2–3 weeks and can be considered negligible for most brachytherapy fractionation schemes

- Reoxygenation—The process of reoxygenation may be rapid; however, complete reoxygenation after large single doses may not be as effective as multiple small fractions
- Radiosensitivity effects, if present, are more likely dependent on fraction number and/or dose rate than the interval between fractions

Timing with EBRT

- Given the effects of repopulation beginning after several weeks of treatment, it is important to not allow a prolonged break from treatment prior to initiation of brachytherapy
- Brachytherapy treatments can be given before the completion of external beam radiation therapy. In these cases, it is important to consider the cumulative dose of radiation on a daily and weekly basis to the tumor and normal tissues. This can be calculated using BED and EQD_2 equations
- It is not recommended to give both EBRT and brachytherapy treatments on the same day to ensure enough time is allowed for repair of sublethal damage in normal tissue

Modeling the Dose Response

Effect of Varying the Dose Size

BED Equations

- Using the linear quadratic equation, it is possible to estimate the biological effect of changing the fraction size of the delivered radiation using a concept first proposed by Dr. Jack Fowler [7]. This is the Biologically Effective Dose (BED)

- Its goal was to illustrate the effect of changing fraction size on the likely effectiveness of the new fractionation scheme
- It was derived only as tool to estimate such effects and was never intended to be used to prescribe actual clinical doses

$$\text{BED} = n \times d \times \left(1 + \frac{d}{\alpha / \beta}\right) \tag{2}$$

- Here, using the defined α/β ratio for the tissue and n fractions of d Gy are given. This equation, however, does not account for the effect of repopulation. While this effect may be negligible for treatments less than 3 weeks in duration, it can be significant for longer treatments especially permanent LDR implants
- To account for the effect of repopulation, the equation can be expanded to:

$$\text{BED} = n \times d \times \left(1 + \frac{d}{\alpha / \beta}\right) - \frac{0.693 \times \left(T - T_{\text{k}}\right)}{\alpha \times T_{\text{p}}} \tag{3}$$

- Here, an overall time of T days and repopulation (with a cell doubling time T_{p}) is delayed until day T_{k} of treatment

EQD2 Equations

- In order to provide a more direct basis for comparison, the BEDs calculated above may be readily converted into doses that are equivalent to a conventional fraction scheme using 2 Gy fractions. This is the equivalent dose in 2 Gy fractions (EQD_2) equation
- This conversion generates doses that are comparable to those seen using conventional 2 Gy per day fractions

$$\text{EQD}_2 = n \times d \times \left(\frac{d + (\alpha / \beta)}{2 + (\alpha / \beta)}\right) \tag{4}$$

- This equation can be used when both external beam and IGBT are being employed in order to generate a composite dose for comparison

Radiobiological Effects of Large Single Doses

- In the context of IGBT, the use of refined imaging techniques to locate both the tumor and organs at risk has enabled the delivery of larger fraction sizes to better defined target areas
- This development, matching changes in the delivery of external beam radiation, has raised questions over the utility of the LQ formula as being the most appropriate tool as it predicts a continuously bending cell survival curve at elevated doses rather than a simple exponential that is normally observed
- This will have the effect of overestimating the potency of LQ-based calculations of BED or EQD_2
- To address this discrepancy, two groups of thought have emerged. One group proposes the continued use of the LQ formulae, citing its long and successful use in the clinic [8]. Others have advised caution, suggesting that the LQ formula does not adequately model biological effects at high doses, such as the introduction of damage to the vascular system [9]
- For this reason, models such as the Universal Cell Survival Curve (USC) have been described that address the practical reality by adding an exponential dose–response element to the LQ model [10]
- Such models, however, negate the biological rationale of using the LQ formulae and its BED and EQD_2 derivatives though not necessarily its practical utility

References

1. Garcia-Barros M, Paris F, Cordon-Cardo C, Lyden D, Rafii S, Haimovitz-Friedman A, et al. Tumor response to radiotherapy regulated by endothelial cell apoptosis. Science (New York, NY). 2003;300(5622):1155–9.
2. Mariotti LG, Pirovano G, Savage KI, Ghita M, Ottolenghi A, Prise KM, et al. Use of the gamma-H2AX assay to investigate DNA repair dynamics following multiple radiation exposures. PLoS One. 2013;8(11):e79541.
3. Hall EJ, Giaccia AJ. Radiobiology for the radiologist. Philadelphia: Wolters Kluwer Health; 2012.
4. Withers HR, Taylor JM, Maciejewski B. The hazard of accelerated tumor clonogen repopulation during radiotherapy. Acta Oncol (Stockholm, Sweden). 1988;27(2):131–46.
5. Steel GG, McMillan TJ, Peacock JH. The 5Rs of radiobiology. Int J Radiat Biol. 1989;56(6):1045–8.
6. Deacon J, Peckham MJ, Steel GG. The radio responsiveness of human tumours and the initial slope of the cell survival curve. Radiother Oncol. 1984;2(4):317–23.
7. Fowler JF. 21 years of biologically effective dose. Br J Radiol. 2010;83(991):554–68.
8. Brown JM, Carlson DJ, Brenner DJ. The tumor radiobiology of SRS and SBRT: are more than the 5 Rs involved? Int J Radiat Oncol Biol Phys. 2014;88(2):254–62.
9. Park HJ, Griffin RJ, Hui S, Levitt SH, Song CW. Radiation-induced vascular damage in tumors: implications of vascular damage in ablative hypofractionated radiotherapy (SBRT and SRS). Radiat Res. 2012;177(3):311–27.
10. Park C, Papiez L, Zhang S, Story M, Timmerman RD. Universal survival curve and single fraction equivalent dose: useful tools in understanding potency of ablative radiotherapy. Int J Radiat Oncol Biol Phys. 2008;70(3):847–52.

Chapter 2
General Physics Principles in Brachytherapy

Sang-June Park and David H. Thomas

Classifications of Brachytherapy

Types of Brachytherapy Implants

- Interstitial: Radiation sources or catheters are surgically inserted into or near the targets (e.g., prostate, gynecological, breast, rectum, and head and neck cancer)
- Intracavitary: Radiation sources are placed into the body cavity in close proximity to the target tissue using applicators (e.g., breast balloon applicators, gynecological vaginal cylinders, multichannel vaginal balloon applicators, tandem and ovoids, tandem and ring, endometrial Y applicator, and rectum mold applicator, etc.)
- Intracavitary + Interstitial hybrid, GYN: Intracavitary hybrid applicators (e.g., tandem and ovoids with

S.-J. Park, PhD (✉)
Department of Radiation Oncology, University of California, Los Angeles, 200 UCLA Medical Plaza, Suite B265, Lost Angeles, CA 90095, USA
e-mail: spark@mednet.ucla.edu

D.H. Thomas, PhD
Department of Radiation Oncology, University of Colorado Denver, 1665 Aurora Ct, Campus Mail Stop F706, Aurora, CO, USA
e-mail: david.h.thomas@ucdenver.edu

J. Mayadev et al. (eds.), *Handbook of Image-Guided Brachytherapy*, DOI 10.1007/978-3-319-44827-5_2

interstitial needles through the ovoids (Utrecht applicator, Elekta, Veenendaal, The Netherlands) and tandem and ring with interstitial needles through the ring (Vienna applicator, Elekta), tandem and ovoids/ring with interstitial needles through the ring combined with interstitial template (Venezia applicator, Elekta)), or a freehand hybrid placement of supplemental needles with a standard intracavitary applicator

- Interstitial + Intracavitary, Breast: Single-entry hybrid applicators placed in the lumpectomy cavity for accelerated partial breast irradiation (e.g., Strut Adjusted Volume Implant (SAVI, Cianna Medical, Aliso Viejo, CA, USA), ClearPath (North American Scientific, Chatsworth, CA, USA), Contura, and MammoSite (Hologic, Bedford, MA, USA) applicators)
- Surface/contact: Radiation sources are inserted into applicators positioned on a skin surface lesion (e.g., tungsten shielded skin applicators with and without flattening filter, the Freiburg flap (Elekta), end Catheter Flap set (Varian, Palo Alto, CA, USA), custom-mold applicators, plaque applicators, surface electronic brachytherapy applicators (Elekta Esteya® system; and iCAD Xoft® system, Nashua, NH, USA))
- Intraluminal: Sources are loaded into a lumen to treat its surface and adjacent tissue (e.g., esophageal, tracheal, bronchial tubes, bile duct applicator)
- Intravascular: Sources are brought intravascularly into or near a lesion
- Intraoperative: Sources are brought surgically into the tumor bed or near the tumor volume (e.g., Harrison-Anderson-Mick (HAM) applicator (Mick Radio-Nuclear Instruments, NY), Freiburg flap applicator (Elekta), the intrabeam system (Carl Zeiss, Oberkochen, Germany), the Axxent® electronic brachytherapy system (Xoft®, iCAD, Nashua, NH, USA))
- Figure 2.1 summarizes the main types of brachytherapy implants

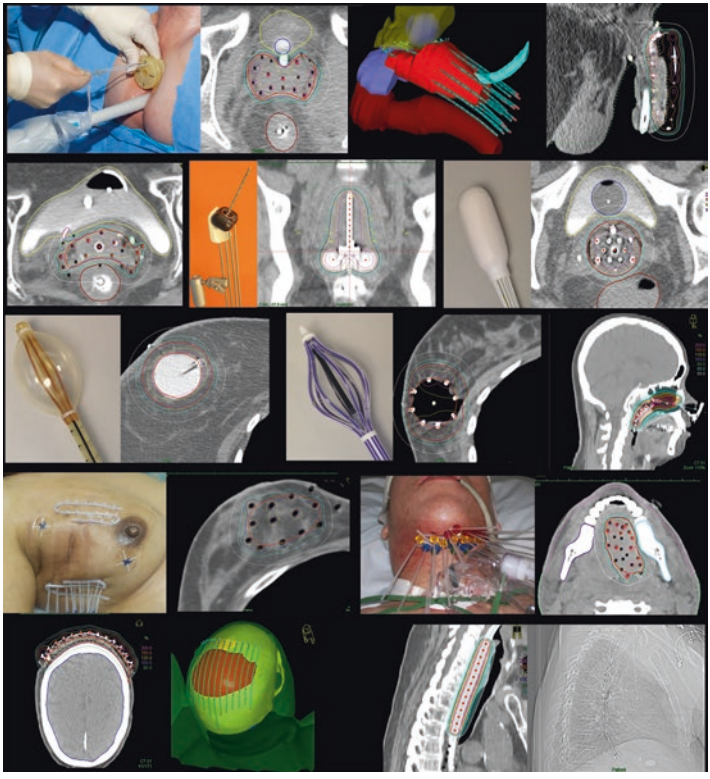

FIG. 2.1. Types of brachytherapy implant. From *left* to *right*, prostate interstitial brachytherapy CT image, implant photo, prostate 3D image, and penile interstitial in the *first row*; gynecological interstitial, tandem and ovoid applicator and CT image, Capri™ vaginal balloon applicator (Varian Medical Systems, Palo Alto, CA, USA), and CT in the *second row*; Contura® breast balloon applicator (Hologic, Bedford, MA, USA) and CT, SAVI applicator (Cianna Medical Group, Aliso Viego, CA, USA) and CT, and nasopharynx intracavitary CT image in the *third row*; breast interstitial (breast tube and button) CT image and photo, head and neck interstitial for base of tongue and implant photo in the *fourth row*; surface/contact brachytherapy for skin (scalp) and 3D image, and esophagus intracavitary CT and scout images in the *fifth row*

Types of Implant Duration

- Temporary implant: Dose is delivered over a period of time that is short in comparison with the half-life of the radiation sources. Sources are removed when the prescribed dose has been reached
- Permanent implant: Dose is delivered over the lifetime of the sources. The sources undergo complete radioactive decay

Types of Source Loading

- Preloading or hot loading: The applicator is preloaded and contains radioactive sources at time of placement into the patient
- Afterloading: The applicator is placed first into the patient, and the radioactive sources are loaded later either by hand (manual afterloading) or by computer controlled machine (automatic remote afterloading) to minimize radiation exposure to hospital personnel

Types of Dose Rate

- Very low dose rate (VLDR): <0.4 Gy/h
- Low dose rate (LDR): 0.4–2 Gy/h
- Medium dose rate (MDR): 2–12 Gy/h
- High-dose rate (HDR): >12 Gy/h [1]
- Pulsed dose rate (PDR) delivers the dose in a large number of small fractions with short intervals in order to achieve a radiobiological effect similar to low dose rate over the same treatment time. PDR treatments are delivered on the same hardware and applicators as the HDR modality [2–4]

Radioactive Sources

Characteristics of Radioactive Source

- Half-life: The time required for the source strength to decay to half of its initial value
- Specific activity: The amount of radioactivity for a given mass of the radioactive source
- Energy spectrum: The energies and types of the radiation particles that are emitted from the source
- Half value layer: Thickness of the material required to decrease the intensity of the incident beam to half of its original value
- Exposure rate constant (Gamma ray constant): The exposure in R/h at a point 1 cm from a 1 mCi point source

Ideal Radioisotopes for Brachytherapy

- Easily available inexpensive materials
- Easily filter emitted charged particles or the absence of charged particle emission
- No gaseous decay product to avoid source contamination by leaking
- Moderate half-life for minimal decay correction during treatment
- Moderate gamma ray constant which determines activity, output, and shielding requirements
- High specific activity to produce smaller size sources with higher output
- Nontoxic and insoluble materials

Source Forms

- Needles, tubes, wires, seeds, cylinder, spherical, beads, pellets, and micro pellets

Brachytherapy Radioisotopes

- Photon sources emit gamma rays through gamma decay and possibly characteristic x-rays through electron capture and internal conversion
- Beta sources emit electrons following beta decay
- Neutron sources emit neutrons following spontaneous nuclear fission reaction
- Historical sources: ^{222}Rn and ^{226}Ra
- Currently used sources: ^{32}P, ^{60}Co, ^{90}Sr/^{90}Y, ^{103}Pd, ^{125}I, ^{137}Cs, ^{192}Ir, and ^{198}Au, and electronic brachytherapy sources [5]
- Developmental sealed sources: ^{131}Cs, ^{145}Sm, ^{169}Yb, ^{241}Am, and ^{252}Cf
- Table 2.1 summarizes physical characteristics of brachytherapy radioisotopes

Treatment Planning

Historically, dosimetry systems such as the Manchester, Paris, Quimby, and Stockholm systems were derived from rich clinical experience used to deliver a specified dose to the tumor accurately in the absence of computerized treatment planning systems.

Dosimetric Systems

- Dosimetric systems are a set of rules to deliver a defined dose to a designated region
- Prior to the development of computerized treatment planning techniques, several classical implant systems were developed to calculate, for a given target volume
  - The total activity of the sources
  - Number of sources
  - The source distribution within the target volume
- Each system is specific to a radioisotope and its spatial distribution within the applicator

TABLE 2.1 Brachytherapy radioisotopes and characteristics

Radionuclide	Half-life	Average energy (MeV)	HVL (mm-lead)	Exposure rate constant (R cm^2 mCi^{-1} h^{-1})
High energy photon sources				
^{60}Co	5.25 years	1.25	11.0	13.07
^{137}Cs	30.0 years	0.662	6.2	3.26
^{192}Ir	73.8 days	0.38	2.5	4.69
^{198}Au	2.7 days	0.412	3.3	2.35
^{222}Rn	3.83 years	0.83	12	8.25
^{226}Ra	1600 years	0.83	14	8.25
Low energy photon sources				
^{103}Pd	17.0 days	0.021	0.0085	1.48
^{125}I	59.4 days	0.028	0.025	1.46
^{131}Cs	9.96 days	0.030	0.022	0.64
Beta sources				
^{32}P	14.3 days	0.695	–	–
$^{90}Sr/^{90}Y$	28.9 years	0.564	–	–
Developmental sources				
^{145}Sm	340 days	0.043	0.060	0.885
^{169}Yb	32 days	0.093	0.48	1.80
^{241}Am	432 years	0.060	0.12	0.12
^{252}Cf	2.65 years	2.1 neutron	–	–

- Each system therefore specifies the following:
  - Type of radioisotope to be used
  - The geometrical arrangement of radioisotope
  - Explicit details of the treatment including dose, time, and administration

- Usually, a system provides a set of tables to allow simple and reproducible calculation in most of the encountered clinical scenarios
- These classical systems have, for the most part, been replaced by computerized treatment planning systems, but remain useful as tools of independent quality assurance (QA) of the computer treatment plans

Manchester System or Paterson–Parker System for Interstitial Implants

- Paterson and Parker developed the Manchester system in 1934 [6, 7]
- The aim of this system is to deliver a uniform dose (within ±10 % from the prescribed dose) within a volume or planar implant
- In order to deliver homogeneous dose distribution, sources are distributed nonuniformly with more source strength concentrated in the periphery of the target volume in comparison to the center
- Different linear activities, 0.33, 0.50, and 0.66 mg Ra/cm radium source, were used
- The use of a specific pattern of distribution of radioactivity was recommended depending on the shape (linear, planar, and volume implant) and size of the implant
- Crossing needles are required to enhance dose at implant ends
- If the implants are not closed-ended or the shape of the implant is not square, the source strength should be adjusted
- The single-plane source arrangement implant is used to treat 1 cm thick slab of tissue, with the dose prescribed to a 0.5 cm away from the source plane
- For thicker slabs, two parallel planes are used to treat slabs of tissue with thickness up to 2.5 cm. The required total source strength is equally distributed between the two planes in proportion to their relative areas

Quimby System or Memorial System for Interstitial Implants

- Developed by Quimby in 1932 [8–11]
- A uniform distribution of source strength allows a higher dose in the center of the treatment volume than near the periphery
- Constant intensity (0.5 or 1.0 mg Ra/cm radium source) was used
- To deliver the prescription dose, a system of tables and rules has been generated to provide the total source strength for a uniform distribution of the source activity
- Dose value obtained from the Quimby tables represents the minimum dose within the target volume
- Typically, dose rates used in the Quimby System for patient treatments (60–70 cGy/h) are much higher than the Patterson–Parker (Manchester) system (40 cGy/h)

Paris System for Interstitial Implants

- This system was developed by Pierquin, Dutreix, and Chassagne for ^{192}Ir wire implants in 1960s and 1970s [12, 13]
- The Paris system is used for single and double plane implants
- The source strength (activity/cm) is uniform and identical for all sources in the implant
- Sources are linear and their placements are parallel
- Adjacent sources must be equidistant from each other. Source separation should be determined according to active implant length
- The prescription dose is made to the "central plane," which is perpendicular to the direction of the sources, at the midpoint of the implant
- Since crossing needles are not used, the active source length is 30–40 % longer than the target length
- In volume implants, cross-sectional source distribution forms a series of equilateral triangles or squares

- The reference isodose is 85 % of the average basal dose, which is defined by the minimum dose between the sources

Stockholm System for Intracavitary Implants

- Based on a fractionated course of radiation treatment using ^{226}Ra sources over a period of 1 month with two or three applications [14, 15]
- 60–80 mg radium sources were placed inside the vagina using an intravaginal applicator while 30–90 mg of radium was placed inside uterus using an intrauterine tube
- A total radiation dose of 6500–7100 mg-h was prescribed for the cervical cancer treatment

Manchester System for Intracavitary Implants

- It was published in 1938 by Tod and Meredith (updated in 1953) and remains in use today [16–18]
- Defines treatment in terms of dose to a point representative of the target, and which is anatomically comparable from patient to patient. The dose points should not be in a region of high-dose gradient (i.e., sensitive to small changes in applicator position)
- A "dose-limiting point" Point A was originally defined as 2 cm lateral to the center of the uterine canal and 2 cm superior to the mucosal membrane of the lateral fornix in the plane of the uterus
- Later Point A was redefined to be 2 cm superior to the external cervical os (or cervical end of the tandem) and 2 cm lateral to the cervical canal
- Manchester system can be characterized by the dose to four points;
  - Point A
  - Point B = 5 cm lateral to the mid pelvis. For example, this would be to Point A, when the central canal is not displaced . This could be further from Point A

if the tandem is favoring one side of the pelvis due to anatomy
- Bladder point - the most dependent portion of the foley balloon with 7 cc of contrast
- Rectum point defined as 0.5 cm posterior to the posterior vaginal mucosa at the lower end of the intruterine source or mid vaginal source

- Figure 2.2 shows definition of points A and B
- If the tandem displaced the central canal, Point A moves with the canal, but Point B remains fixed at 5 cm from midline
- 20, 15 – 10, and 15 – 10 – 10 mg of Ra was loaded in the short, medium, and long uterine tubes. 17.5, 20, and 22.5 mg of Ra was loaded in the small, medium, and large ovoids
- Designed such that:
  - Dose rate at Point A was approximately 0.53 Gy/h for all allowed applicator loadings
  - Vaginal contribution to Point A was limited to 40 % of the total dose

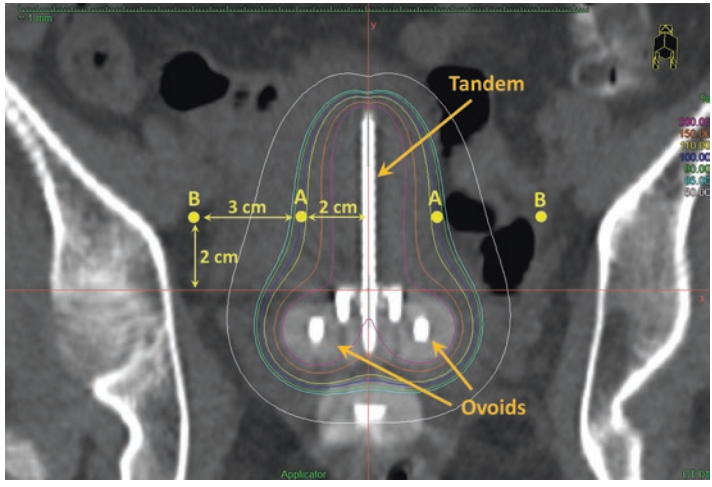

Fig. 2.2. Definition of points A and B for intracavitary implant according to the Manchester system

  - The rectal dose should be 80 % or less of the dose to Point A
  - In the absence of external beam, 80 Gy to Point A was prescribed in two applications with total of 144 h
- In 1938 Tod showed that toxicity to the pyramid shaped area, "paracervical triangle," in the medial edge of the broad ligament (where uterine vessels cross the ureter) was the main dose limiting factor in the treatment of the uterine cervix
- The validity of this point for this was illustrated in a study of over 500 cases, which showed a clear relationship between the tolerance of normal tissues and the dose received to this area

Paris System for Intracavitary Implants

- A single application of radium brachytherapy was prescribed for cervical cancer treatment [12, 13]
- Unlike the Stockholm system, almost an equal amount of radium was used in the uterus and the vagina in the Paris system
- The system used two cork colpostats in the form of a cylinder and an intrauterine tube
- The system was designed to deliver a dose of 7000–8000 mg-h of radium over a period of 5 days
- One intrauterine source contained three radium sources with source strengths in the ratio of 1:1:0.5. The source strength of the topmost uterine source was the same as the strengths in the colpostats

Problems with Older Dosimetric Systems

- Since both the Paris and the Stockholm Systems used intrauterine tubes, which were separate from the vaginal colpostats, these systems had a loose geometry
- With the use of external-beam radiotherapy which specified the prescription in terms of the absorbed

dose, the use of Milligram-hours of radium as a unit in brachytherapy was no longer acceptable
- In addition, dose prescription in this unit ignored the importance of tolerance of different critical organs to radiation. This was because the dose to important anatomical targets could not be quantified adequately with the use of this dose prescription method

Dose Optimization

- Optimization is shaping of the isodose line. Normalization is scaling of the isodose lines
- Goals of optimization:
  - Homogeneous dose distribution in the target
  - Coverage of the target with minimum prescription dose
  - Sparing dose to critical organs with high-dose gradient outside the target
- Optimization methods:
  - Manual dwell weights
  - Manual dwell times
  - Geometrical optimization (distance and volume optimization)
  - Graphical optimization
  - Inverse planning optimization (IPSA, HIPO, etc.)
- Optimization of dose distribution is usually achieved by weighting the relative spatial and temporal distribution of sources in order to achieve the required dose at prescription point/volume coverage
- Source dwell position and relative dwell times are analytically optimized in order to achieve the desired dose distribution
- Typical optimization algorithms initially assign dwell times for all source dwell positions based on their respective distances to each other
- To compensate for the reduced dose contribution from the other dwell positions, a dwell position at larger distance from any other dwell positions will be assigned larger dwell times

- A homogeneous dose distribution, as defined by the ratio of volume of high dose to volume of prescription dose (e.g., dose homogeneity index (DHI) = 1 – V150/V100) will be the result of this initial optimization
- More advanced optimization techniques include graphic optimization and inverse planning optimization
- Graphic optimization allows graphical control over desired isodose lines, with the dwell locations and time updated accordingly
- Inverse planning is an anatomy-based dose distribution optimization approach [19]
- Similarly to IMRT, inverse planning in brachytherapy requires 3D-imaging (CT, MRI, Ultrasound, etc.) and the segmentation (contouring) of Volumes of Interest (VOI)
- Optimized dose distributions should be carefully reviewed to avoid unintended high-dose regions or gradients arising due to control of target/OAR dose distributions

Dose Calculation

Fundamental Problems with Old Dose Calculation Protocols

- Real brachytherapy source gives anisotropic distribution since it is not exactly equivalent to a point source.
- Old protocols calculate photon fluence in free space and do not take into account photon scattering in a scattering medium (tissue)
- For accurate dose calculation in clinical applications, dose distributions should be calculated in a scattering medium (water equivalent medium)

AAPM TG-43 Protocol

The AAPM recommended TG-43 dosimetry protocol to resolve the fundamental problems with the old dose calculation protocols [20, 21]. From the AAPM-TG 43 protocol,

dose rate, $\dot{D}(r,\theta)$ at Point P with polar coordinate (r, θ) in a medium is

$$\dot{D}(r,\theta) = S_K \cdot \Lambda \cdot \frac{G_L(r,\theta)}{G_L(r_0,\theta_0)} \cdot g_L(r) \cdot F(r,\theta)$$

- r: the distance (in centimeters) from the center of the active source to the point of interest
- θ: the angle specifying the point of interest relative to the source longitudinal axis
- r_0: the reference distance which is specified to be 1 cm in this protocol
- θ_0: the reference angle on the source transverse plane and is specified to be 90° or $\pi/2$ radians
- Figure 2.3 shows the geometry used in the dose calculation based on the AAPM-TG 43 protocol
- S_K: air-kerma strength
  - $S_K = \dot{K}_\delta(d)d^2$

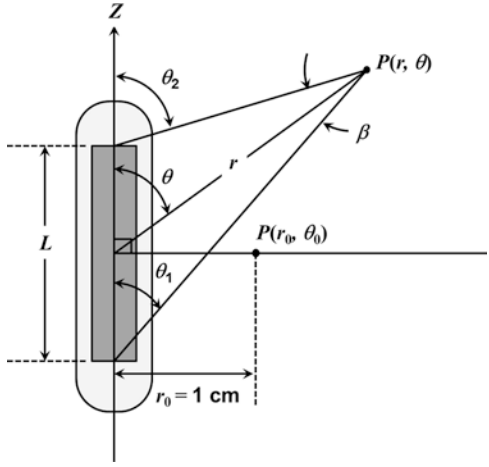

FIG. 2.3. Illustration of geometry used in the TG-43 dose calculation formalism

- air-kerma rate at the point along the transverse axis of the source in free space
- a measure of brachytherapy source strength
- units of 1 U = 1 μ Gy m^2h^{-1} = 1 cGy cm^2h^{-1}
- measured in vacuo meaning that it must not include effects due to attenuation or scattering in a medium
- must be measured at a distance much larger than the source length (typically of the order of 1 m)
- include contributions from photons greater than δ (energy cutoff, typically 5 keV) to exclude low-energy or contaminant photons
- usually determined by an NIST wide angle free air chamber

- Λ: dose-rate constant
  - $\Lambda = \dfrac{\dot{D}\left(r_{0,}\theta_0\right)}{S_K}$
  - the dose rate to water as a distance of 1 cm on the transverse axis of a unit air kerma strength source in a water phantom
  - depends not only on the radioactive material type and quantity but also the source construction
  - $\Lambda = 0.686$ for ^{103}Pd, 0.965–1.036 for ^{125}I, 1.12 for ^{192}Ir.
- $G_L(r, \theta)$: geometry function
  - accounts for the variation of relative dose due to the spatial distribution of activity within the source
  - generalizes the inverse square correction
  - considering the fall-off of the photon fluence
  - ignoring photon attenuation and scattering in the source
  - $$G_L\left(r,\theta\right) = \begin{cases} \dfrac{\beta}{Lr\sin\theta} & if \quad \theta \neq 0° \\ \left(r^2 - L^2/4\right)^{-1} & if \quad \theta = 0° \end{cases}$$

    line-source approximation
  - $G_P\left(r,\theta\right) = r^{-2}$ point-source approximation

- $g_L(r)$: radial dose function
  - $$G_L(r) = \frac{\dot{D}(r, \theta_0)}{\dot{D}(r_0, \theta_0)} \frac{G_L(r_0, \theta_0)}{G_L(r, \theta_0)}$$
  - accounts for the effects of absorption and scatter in the medium along the transverse axis of the source
  - Figure 2.4 shows the radial dose functions for the most commonly used brachytherapy sources
- $F(r, \theta)$: 2D anisotropy function
  - $$F(r,\theta) = \frac{\dot{D}(r,\theta)}{\dot{D}(r, \theta_0)} \frac{G_L(r_0, \theta_0)}{G_L(r, \theta_0)}$$
  - accounts for the anisotropy of dose distribution around the source
  - including the effects of absorption and scatter in the medium
  - Figure 2.5 shows anisotropy function for ^{192}Ir source

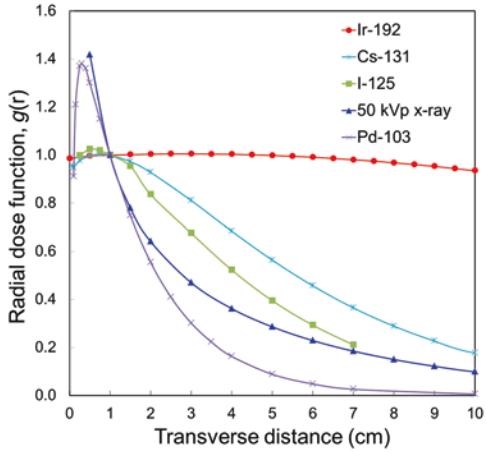

FIG. 2.4. Radial dose functions in water for ^{103}Pd, 50 kVp x-ray, ^{125}I, ^{131}Cs, and ^{192}Ir sources

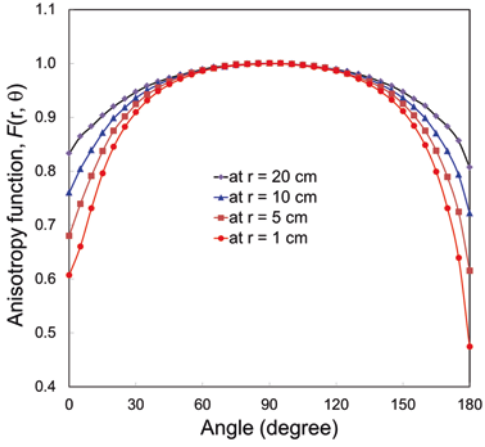

FIG. 2.5. Anisotropy function for ^{192}Ir Flexitron source

- Dose rate at the implant:

$$\dot{D} = \dot{D}_0 \mathrm{e}^{-\lambda t}$$

- Cumulative dose:

$$D_{\mathrm{cum}} = \dot{D}_0 \int_0^t \mathrm{e}^{-\lambda t} dt = \frac{\dot{D}_0}{\lambda}\left(1 - \mathrm{e}^{-\lambda t}\right)$$

- Total delivered dose from short treatment time $\left(t \ll t_{1/2}\right)$:

$$D_{\mathrm{cum}} = \dot{D}_0 \int_0^t \mathrm{e}^{-\lambda t} dt \cong \frac{\dot{D}_0}{\lambda}\left\{1 - \left(1 - \mathrm{e}^{-\lambda t}\right)\right\} = \dot{D}_0 t$$

- Total delivered dose from permanent implant $\left(t \to \infty\right)$:

$$D_{\mathrm{cum}} = \dot{D}_0 \int_0^\infty \mathrm{e}^{-\lambda t} dt = \frac{\dot{D}_0}{\lambda} = \dot{D}_0 \tau$$

- $\dot{D}_0$: initial dose rate (Gy/h)
- $\lambda = \frac{\ln 2}{T_{1/2}}$: decay constant
- $T_{1/2}$: half-life of the radioisotope
- $\tau = \frac{1}{\lambda}$: mean lifetime of the radioisotope

Model-Based Dose Calculation (MBDCA, AAPM TG-186 Protocol)

- Monte Carlo simulations in brachytherapy geometries show errors incurred with the AAPM TG-43 approach [22]
- The significant dose differences in nonwater media (tissues, applicators, and air-tissue interfaces) were seen in the low energy region (<50 keV)
- For the dependence of scatter dose in the 3D geometry, either the radiation transport simulation in the actual media or multiple-dimensional scatter integration is used in the MBDCA approaches

Grid-Based Boltzmann Equation Solvers (GBBS)

- The linear Boltzmann transport equation (LBTE) is the governing equation for radiation transport
- The GBBS are deterministic methods for solving the true continuous LBTE by discretizing the phase-space variables (space, angle, and energy)
- The GBBS was commercially integrated into the Acuros® TPS by Varian Medical Systems

Monte Carlo Simulations (MC)

- In order to solve the LBTE, the MC simulations were used with random sampling

- The MC codes include PTRAN, EGSnrc, MCNP, GEANT4, etc
- In order to the LBTE by random sampling, the MC simulations were used
- The MC is the current state of the art in computational dosimetry, but not optimized for calculation speed
- Pre-calculated phase-space files were used to accelerate calculation speed
- Not commercially available for brachytherapy planning

Collapsed-Cone Superposition/Convolution Method (CCC)

- CC is a point kernel superposition method
- For calculation efficiency, the CCC algorithm uses angular discretization ("collapsed cones") of the kernels along a radiation transport grid
- The primary dose was calculated through a direct ray tracing of the primary photons using the kerma approximation
- The secondary dose from first scatter and multiple scatters was calculated separately with different kernels for heterogeneities
- The CCC algorithm has implemented in the Oncentra® BrachyTPS from Elekta (Veenendaal,The Netherlands)

References

1. International Commission on Radiation Units and Measurements (ICRU). 1985 dose and volume specification for reporting and recording intracavitary therapy in gynecology. Report 38 of ICRU. Bethesda: ICRU Publications.
2. Brenner DJ, Hall EJ, Randers-Pehrson G, Huang Y, Johnson GW, Miller RW, Wu B, Vazquez ME, Medvedovsky C, Worgul BV. Quantitative comparisons of continuous and pulsed low dose rate regimens in a model late-effect system. Int J Radiat Oncol Biol Phys. 1996;34:905–10.

3. Chen CZ, Huang Y, Hall EJ, Brenner DJ. Pulsed brachytherapy as a substitute for continuous low dose rate: an in vitro study with human carcinoma cells. Int J Radiat Oncol Biol Phys. 1997;37:137–43.
4. Visser AG, van den Aardweg GJ, Levendag PC. Pulsed dose rate and fractionated high dose rate brachytherapy: choice of brachytherapy schedules to replace low dose rate treatments. Int J Radiat Oncol Biol Phys. 1996;34:497–505.
5. Williamson JF. Clinical brachytherapy physics. In: Perez CA, Brady LW, editors. Principles and practice of radiation oncology. 3rd ed. Philadelphia: Lippincott Williams and Wilkins; 1998. p. 405–67.
6. Paterson R, Parker HMA. A dosage system for gamma ray therapy. Br J Radiol. 1934;7:592–612.
7. Paterson R, Parker HMA. A dosage system for interstitial radium therapy. Br J Radiol. 1952;25:505–16.
8. Quimby EH. The grouping of radium tubes in packs on plaques to produce the desired distribution of radiation. Am J Roentgenol. 1932;27:18.
9. Quimby EH. Dosage tables for linear radium sources. Radiology. 1944;43:572–7.
10. Quimby EH, Castro V. The calculation of dosage in interstitial radium therapy. Am J Roentgenol. 1953;70:739–49.
11. Glasser O, Quimby EH, Taylor LS, et al. Physical foundations of radiology. 3rd ed. New York: Harper & Row; 1961.
12. Pierquin B. Precis de Curietherapie. Endocurietherapie et Plesiocurietherapie. Paris: Masson; 1964.
13. Pierquin B, Dutreix A, Paine C, Chassagne D, Marinello G, Ash D. The Paris system in interstitial radiation therapy. Acta Radiol Oncol. 1978;17(1):33–48.
14. Heymann J. The so-called Stockholm method and the results of treatment of uterine cancer at Radiumhemmet. Acta Radiol. 1935;16:129–48.
15. Kottmeier HL. Surgical and radiation treatment of carcinoma of the uterine cervix. Experience by the current individualized Stockholm Technique. Acta Obstet Gynecol Scand. 1964;43(2):1–48.
16. Tod M, Meredith WJ. A dosage system for use in the treatment of cancer of the uterine cervix. Br J Radiol. 1938;11:809–24.
17. Tod M, Meredith WJ. Treatment of cancer of the cervix uteri—a revised Manchester method. Br J Radiol. 1953;26:252–7.
18. Meredith WJ. Radium dosage: the Manchester system. Edinburg: Livingston; 1967.

19. Lessard E, Pouliot J. Inverse planning anatomy-based dose optimization for HDR-brachytherapy of the prostate using fast simulated annealing algorithm and dedicated objective function. Med Phys. 2001;28(5):773–9.
20. Nath R, Anderson LL, Luxton G, Weaver KA, Williamson JF, Meigooni AS. Dosimetry of interstitial brachytherapy sources: recommendations of the AAPM Radiation Therapy Committee Task Group No.43. American Association of Physicists in Medicine. Med Phys. 1995;22(2):209–34.
21. Rivard MJ, Coursey BM, DeWerd LA, Hanson WF, Huq MS, Ibbott GS, Mitch MG, Nath R, Williamson JF. Update of AAPM Task Group No. 43 Report: a revised AAPM protocol for brachytherapy dose calculations. Med Phys. 2004;31(3):633–74.
22. Beaulieu L, Carlsson Tedgren A, Carrier JF, Davis SD, Mourtada F, Rivard MJ, Thomson RM, Verhaegen F, Wareing TA, Williamson JF. Report of the Task Group 186 on model-based dose calculation methods in brachytherapy beyond the TG-43 formalism: current status and recommendations for clinical implementation. Med Phys. 2012;39(10):6208–36.

Chapter 3
Treatment Delivery Technology for Brachytherapy

J. Adam M. Cunha and Dae Yup Han

Introduction

Because of the wide range of applications and tumor sites treated with brachytherapy, delivery technology is extremely diverse. Brachytherapy is customizable and allows for personalized design of applicators and implants tailored to each patient. This chapter will summarize the most popular delivery techniques. We will cover a few helpful rules of thumb for the physics and planning of brachytherapy implants. Then, we will cover the most common types of brachytherapy procedures: permanent seed implants and afterloader-based temporary implants. Finally, we will discuss microsphere brachytherapy.

J.A.M. Cunha, PhD (✉) • D.Y. Han, PhD
Department of Radiation Oncology, University of California, San Francisco, 1600 Divisadero St, Box 1708, Suite H1030, San Francisco, CA 94115, USA
e-mail: Adam.Cunha@ucsf.edu; DaeYup.Han@ucsf.edu

J. Mayadev et al. (eds.), *Handbook of Image-Guided Brachytherapy*, DOI 10.1007/978-3-319-44827-5_3

General Physics and Technology

- Inverse r-squared law results in quick fall off of dose
- As a rule of thumb, the 50 % isodose line is separated from the 100 % isodose line by a distance of approximately 1 cm. This is a useful point of reference when estimating expected dose to organs at risk
- As a rule of thumb, the half-life of the Ir-192 sources used most commonly for high dose rate (HDR) brachytherapy will cause a drop in activity of approximately 1 % per day
- Temporary implants result in no radiation being left in the patient when they leave the clinic/hospital. Permanent implants do leave radioactive material in the patient
- A vast database of information on brachytherapy sources can be found at the web site of the Imaging and Radiation Oncology Core (IROC) at M.D. Anderson Cancer Center (http://rpc.mdanderson.org). This database, the Joint AAPM/IROC Houston Registry of Brachytherapy Sources Meeting the AAPM Dosimetric Prerequisites, includes both currently available sources and older sources no longer available
- Forward-based planning, e.g., Point-A-based cervical brachytherapy has been a standard of brachytherapy for decades, but its use has been falling out of favor over the last decade due to the target dose coverage and normal tissue dose sparing techniques available with modern inverse planning techniques. Inverse planning uses anatomical information to inform the dose distribution. Inverse Planning Simulated Annealing (IPSA) was one of the first widely implemented inverse planning systems for brachytherapy [1–3]
- Specialized clinics may produce custom applicators for each patient and modern additive manufacturing (3D printing) techniques can be especially useful. If custom materials are used for patient-specific applicators; however, it is critical to understand the dosimetric properties of the fabrication materials for the photon energy range of the source being used [4, 5]

Permanent Implant Brachytherapy

General Facts

- Most common uses: Prostate, Brain
- Typical dose rate at time of implant: 0.4–2.0 Gy/h.
- Treatment dose delivered on a timescale of weeks/months.
- Radiation dose rate decays to background in approximately 5 half-lives
- No shielding required for implant room
- Exposure to physicists and physicians during preparation and implant is low but non-zero
- Seeds may be ordered loose or in preloaded needles
- Radiation sources are placed within or on the cancer volume and left in place indefinitely
- Because the radiation is left in the patient after discharge, security scans will pick up a signal above background for the first few months. UCSF gives each patient an identification card to provide to, e.g., airport security (Fig. 3.1).

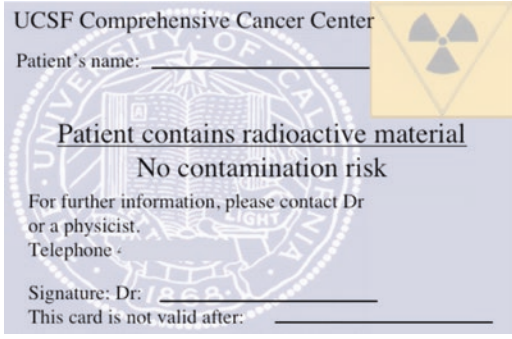

Fig. 3.1. Radiation card. The identification card provided by UCSF for each patient after a procedure that places radioactive material in the body permanently. This card should be carried by patients to be shown, e.g., to airport security

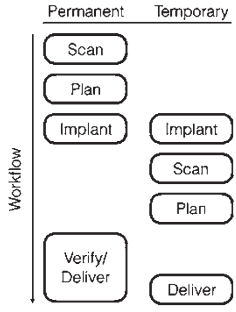

FIG. 3.2. Workflow. The implant workflow for the two most common sealed source brachytherapy delivery types: permanent seed implants and afterloader-based (temporary, HDR) implants. Permanent implants are commonly called low dose rate implants, while temporary implants can be either low dose rate or high dose rate. The main difference is the timing of the dose planning, which is done prior to the implant procedure for permanent case and after the catheter insertion procedure for the temporary implant case

Workflow

- The standard workflow for permanent prostate implants is: Scan, Plan, Implant, Verify (S-P-I-V). Figure 3.2 shows the difference between the workflow for permanent implants and temporary brachytherapy treatment like high dose rate brachytherapy
- *Scan*—The pre-implant scan is generally done under the same conditions as will be present for the implant. This is generally trans-rectal ultrasound
  - Often called a *volume study*
  - Performed several days to a few weeks prior to implant to allow time for dose planning and seed ordering/delivery
  - MR spectroscopy in prostate may be used to identify local lesions

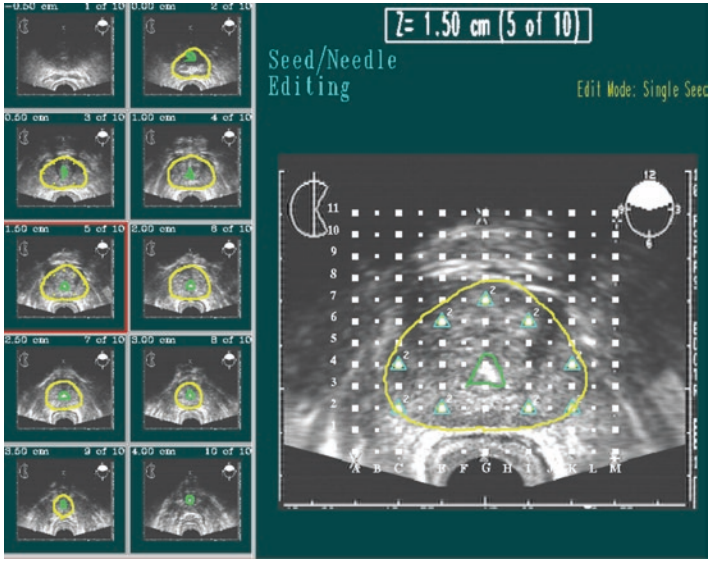

FIG. 3.3. Template. A pre-implant plan for a prostate permanent-seed implant. Note the *grid of white dots* corresponds to the needle insertion grid placed on the perineum of the patient. This is co-registered with the trans-rectal ultrasound used to obtain the image

- *Plan*—Planning is done using the pre-implant scan and planning software specifically designed for the task. The template grid used for needle insertion is overlaid on the ultrasound image to provide a 3D matrix of seed placement locations typically 0.5 cm in the left-right and anterior-posterior directions, and 5 cm in the superior-inferior direction (Fig. 3.3)
  - Often referred to as the *preplan* since it is done prior to the implant (contrast with the afterloaded brachytherapy workflow)
  - Generate a dose plan based on the image set obtained.
  - Planning may be done manually or with inverse planning

- Seed order-to-delivery times are approximately 1 week
- Seeds my come preloaded in needles ready for implant or loose. If they are ordered loose, the medical physicist is responsible for loading each needle with the correct seed configuration

- *Implant*—The needle template used to guide the needle insertion is placed on the perineum and the current (live) ultrasound implant is aligned with the preplan scan. This co-registers the planned prostate volume with the position of the prostate at the time of the surgical procedure
  - Done under anesthesia in an operating room
  - Typical time: 1 h
  - After the procedure, the patient generally takes 1–3 h to recover from anesthesia at which point they are able to leave the hospital
- *Verify*—Post-implant dosimetry is required to verify the placement of the seeds and to record the dose delivered to the patient
  - Most commonly done using CT imaging
  - Up to 30 days after the implant but can be done on the day of the implant. If done on the day of the implant, edema needs to be accounted for since it will cause the dose coverage to appear cooler (Fig. 3.4) [6].
- The workflow for brain or other implants that do not incorporate pre-implant planning is simpler: Steps 1-Scan and 2-Implant are not performed. A number of seeds are ordered prior to the operation based on the expected size of the resection cavity. The implant immediately follows surgical resection of the bulky mass of the tumor in the operating room. After surgical resection of the tumor, the seeds are glued one-by-one to the inner surface of the resection cavity in an approximately 1 cm × 1 cm grid. A post-implant CT scan is obtained to perform the dosimetry of the implant and recorded in the patient's medical record

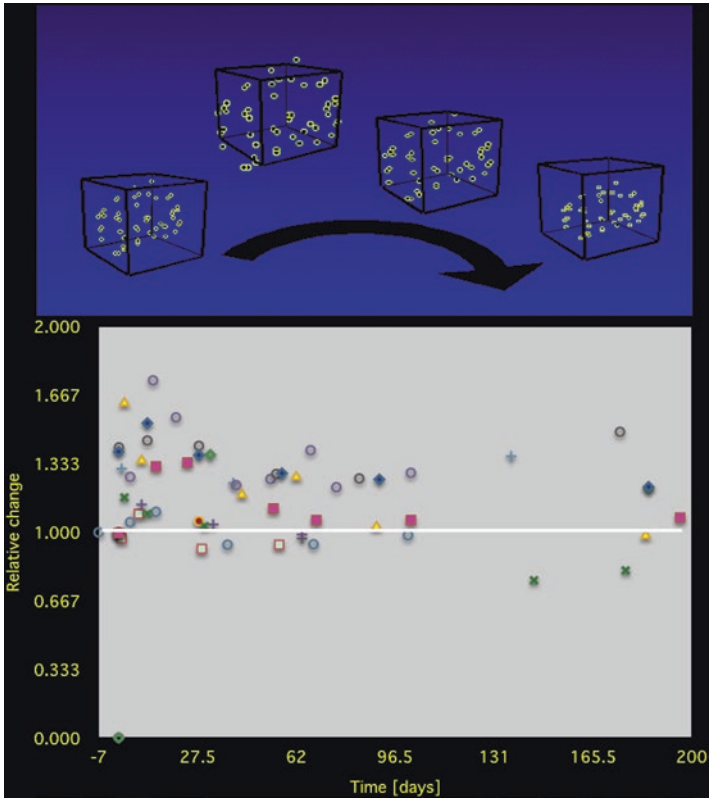

FIG. 3.4. Edema. Prostate edema as a function of time after a permanent implant for a sample of 10 randomly selected patients from our clinic. While edema doesn't have a significant effect for all patients, it can cause an increase in the volume of the prostate by a factor of two. This can have a significant impact on the dose delivered to the gland

Table 3.1 Common PPI sources: the three most commonly used sealed brachytherapy sources for permanent implants

Radionuclide	Half-life (days)	Average energy (keV)	Year introduced	Typical monotherapy seed strength (mCi)	(U)
125-I	59.4	28.4	1965	0.3–0.6	0.4–0.8
103-Pd	17.0	20.7	1986	1.1–2.2	1.4–2.8
131-Cs	9.7	30.4	2004	2.5–3.9	1.6–2.5

Common Radionuclides

The three most common radionuclides for permanent implants are Iodine-125, Palladium-103, and Cesium-131 (Table 3.1).

- 125-I
  - Decay: γ-ray emitting, characteristic X-rays are produced by e^- capture
  - Average energy: 0.028 MeV
  - Half-life: 60 days
  - Half value layer (lead): 0.02 mm
  - Commonly used in clinic with hot loading
- 103-Pd
  - Decay: e^- capture with emission of characteristic X-rays, γ ray emitting
  - Average energy: 0.021 MeV
  - Half-life: 17 days
  - Half value layer (lead): 0.01 mm
  - Commonly used in clinic with hot loading
- 131-Cs
  - Decay: Electron capture with emission of characteristic X-rays and electrons. Electrons are absorbed in seed wall.
  - Average energy: 0.029 MeV
  - Half-life: 9.7 days
  - Half value layer (lead): 0.03 mm

- Source models: Sources are manufactured by a number of different vendors. The design of each source is different for each vendor as can be seen in Fig. 3.5a, b.

Afterloader-Based Brachytherapy

General Facts

- The main advantage of afterloader-based brachytherapy is that is simple utilize time as a treatment planning variable
- Minimum dwell times are generally 0.1 s with typical dwell times ranging from 0.1 to 60 s or longer
- Typical dose rate: 12 Gy/h or more [7]
- Typical treatment times are on the order of 10 min
- Shielding:
  - Linac vault design is sufficient for HDR brachytherapy;
  - CT room design is NOT sufficient for HDR brachytherapy
- Cancer site use:
  - Common: prostate, gynecologic, breast, skin
  - Less common: oral cavity, base of tongue, nasopharynx, bronchial, kidney, keloids
  - No sites are explicitly contraindicated
  - Main restriction on site use is accessibility via intracavitary applicator or interstitial needle

Workflow

The standard workflow for afterloader-based brachytherapy is: Implant, Scan, Plan, Deliver (I-S-P-D). The procedure is described in detail in the report of AAPM Task Group 59 [8] and is illustrated in Fig. 3.6.

- *Implant*—Applicators are chosen depending on the tumor site being treated. Figure 3.7a–h shows some of